





A space-time multigrid method for poroelasticity equations with random hydraulic conductivity

Sebastião Romero Franco^a  and Marcio Augusto Villela Pinto^b 

^aDepartment of Mathematics, State University of Centro-Oeste, Irati, Paraná, Brazil; ^bDepartment of Mechanical Engineering, Federal University of Paraná, Curitiba, Paraná, Brazil

ABSTRACT

In this work, we propose a space-time multigrid method for solving a finite difference discretization of the linear Biot's model in two space dimensions considering random hydraulic conductivity. This method is an extension of the one developed by Franco et al. [1] and which was applied to the heat equation. Particularly for the poroelasticity problem, we need to use the Tri-Diagonal Matrix Algorithm (TDMA) for systems of equations with multiple variables (block TDMA) solver on the planes xt and yt with zebra-type wise-manner (the domain is divided into planes and solve each odd plane first and then each even plane independently [2]). On the planes xy , the F-cycle multigrid with fixed-stress smoother is improved by red-black relaxation. A fixed-stress smoother is compound solver, where the mechanical and flow parts are addressed by two distinctive solvers and symmetric Gauss-Seidel iteration. This is the basis of the proposed method which does not converge only with the standard line-in-time red-black solver [1]. This combination allows the code parallelization. The use of standard coarsening associated with line or plane smoothers in the strong coupling direction allows an application in real world problems and, in particular, the random hydraulic conductivity case. This would not be possible using the standard space-time method with semicoarsening in the strong coupling direction. The spatial and temporal approximations of the problem are performed, respectively, by using Central Difference Scheme (CDS) and implicit Euler methods. The robustness and excellent performance of the multigrid method, even with random hydraulic conductivity, are illustrated with numerical experiments through the average convergence factor.

ARTICLE HISTORY

Received 4 April 2023
Revised 30 August 2023
Accepted 18 September 2023

KEYWORDS

Biot's model; fixed-stress; random coefficients; standard coarsening

PACS

PACS 02.60.Cb; PACS 02.70.Bf; PACS 47.56.+r; PACS 91.60.Np

MATHEMATICS SUBJECT CLASSIFICATION (2020)

MSC 65F10; MSC 65M06; MSC 65M22; MSC 65M55

1. Introduction

The poroelasticity equations mathematically model the interaction between the deformation of a porous elastic material and the fluid flow within it [3]. Nowadays, the analysis and numerical simulation of the Biot consolidation model have become increasingly popular due to the wide range of applications of poroelasticity theory in different branches of research of Science and Engineering such as Medicine, Biomechanics, Petroleum Engineering, Food Processing, etc. Computational mathematics aspects of flow and mechanics of porous media can be seen in several papers of the special issue of Vermolen et al. [4].

This problem can be formulated as a time-dependent coupled system of partial differential equations (PDEs) with the pressure of the fluid and displacements of the solid matrix as

unknowns. Solving such problems analytically is a complicated and sometimes impossible task. Therefore, its numerical solution is an option [5].

Other problems of great interest, such as problems involving wave propagation, thermo-poroelasticity, viscoelastic representation, infinituple-porosity media, Navier-Stokes and bioheat equations, also share the same difficulty [6–11].

Among the various discretization methods, there is the Finite Difference Method (FDM) [5]. The FDM with staggered grids and the implicit Euler method to temporal variables was described by Gaspar et al. [12].

Multigrid methods are among the most efficient techniques for solving large systems of equations arising from the discretization of PDEs and can achieve convergence rates independent of the problem size [13, 14]. Its convergence strongly depends on the choice of the algorithm components [13, 15]. In particular, it is crucial to find a good interplay between the smoothing method and the coarse-grid correction algorithm.

The multigrid method has been used for a long time to solve PDE systems, as described in [2, 16, 17]. In Gaspar et al. [18] was presented a robust and efficient smoother for a transformed version of the system of poroelasticity equations with an additional stabilization term that allows treating the system in an uncoupled way. In Gaspar and Rodrigo [19] was shown the fixed-stress split method to obtain an efficient solver for Biot's problem that decouples the flow from the mechanical part in the smoothing algorithm and in Luo et al. [20] was used a monolithic multigrid method together with either a coupled Vanka smoother [21] or a decoupled Uzawa smoother [22] as an efficient numerical technique for the linear discrete system obtained by finite volumes on staggered grids.

There are other smoothers that can be associated with the multigrid method, such as the zebra-type method [1]. The zebra-type smoothers (or relaxation planes) consist of dividing the domain into planes and first solve each odd plane and then each even plane independently [2].

In search of more efficient methods and taking advantage of the new generation of supercomputers, then one must develop algorithms which are capable to efficiently use large number of cores. However, the classical approach (time-stepping) [19] does not allow the parallelization of the temporal variable. This led us to look for different multigrid approach on time-parallel and full space-time methods [1, 23–29].

In this work, we develop algorithms with zebra-type smoother, for multigrid method, capable of efficiently using large numbers of cores. The results obtained in this current study indicate that the proposed methodology is promising in the sense that we have presented an efficient, robust, and highly parallelizable multigrid method to obtain good convergence factors considering random hydraulic conductivity. For this, we use multigrid method based on a space-time approach with standard coarsening, the block TDMA method to directly solve each of the planes xt and yt and a block zebra-wise manner (also using multigrid) to approximate the solution of the spatial planes.

The remainder of this paper is organized as follows: in Sect. 2, we present the mathematical and numerical models; in Sect. 3, we explain the theoretical foundation necessary about coarsening and smoothing strategy for the comprehension of this paper; in Sect. 4, we show the results, and finally; in Sect. 5, we present the conclusions.

2. Mathematical and numerical models

2.1. Mathematical model

In this paper, we present the two-dimensional Biot's model, on the spatial domain $\Omega = (0, 1) \times (0, 1)$, which can be formulated as a coupled system of PDEs for the unknowns displacements of the solid matrix, u , and pore pressure of the fluid, p . Following this notation, the

governing equations read as follows [30],

$$\nabla(\lambda + \mu)\nabla \cdot \mathbf{u} + \nabla \cdot \mu\nabla\mathbf{u} - \alpha\nabla p = \mathbf{f}(\mathbf{x}, t), \tag{1}$$

$$\frac{1}{\beta} \frac{\partial p}{\partial t} + \alpha \frac{\partial}{\partial t}(\nabla \cdot \mathbf{u}) - \nabla \cdot (k(\mathbf{x})\nabla p) = g(\mathbf{x}, t), \tag{2}$$

where $\mathbf{x} = (x, y) \in \Omega = (0, 1) \times (0, 1)$, $t \in [0, T]$ where T is the period or final time, $\lambda = \frac{\nu E}{(1+\nu)(1-2\nu)}$ and $\mu = \frac{E\nu}{2(1+\nu)}$ are the Lamé coefficients, given in terms of the Young’s modulus E and the Poisson ratio ν . β is the Biot modulus, α is the Biot–Willis fluid/solid coupling coefficient, $k(x, y)$ is the hydraulic conductivity, \mathbf{f} is the density of applied body forces and g represents a forced fluid extraction or injection process.

To complete the formulation of a well-posed problem we must add appropriate boundary and initial conditions. Considering $\mathbf{u} = (u, v)$, $\mathbf{f} = (f_1, f_2)$ and assuming the rigid (zero displacement) and permeable (free drainage) boundary, $\partial\Omega$, such that one has, for simplicity, the boundary and the initial conditions satisfying null solution.

2.2. Numerical model

We consider the spatial domain as a porous medium with random hydraulic conductivity. For the discretization, we consider a uniform space-time grid on $\Omega \times [0, T]$, given by $G_{h,\tau} = G_h \times G_\tau$, where G_h and G_τ represent the spacial and temporal discretizations, respectively, given by

$$G_h = \{ x_{i,j} = (ih, jh) \mid i = 0, \dots, n_x, j = 0, \dots, n_y \} \tag{3}$$

and

$$G_\tau = \{ t_k = kt \mid k = 0, \dots, n_t \}, \tag{4}$$

being the discretization parameter $h = \frac{1}{n_x} = \frac{1}{n_y}$ for both dimensions and G_τ is defined as $\tau = \frac{T}{n_t}$. A standard collocated finite difference scheme on such a grid, together with a stabilization term to avoid unphysical oscillations, is considered. More concretely, the additional term looks like a temporal derivative of a Laplacian of the pressure $\frac{\partial \Delta p}{\partial t}$ which is multiplied by the stabilization parameter $-\frac{h^2}{4(\lambda+2\mu)}$ in Eq. (2) (see [18, 31]), i.e. the additional smoothing term is $-\frac{h^2}{4(\lambda+2\mu)} \frac{\partial \Delta p}{\partial t}$.

The numerical model uses the second order CDS for spatial variables, implicit Euler method for temporal approximation and the additional smoothing term on the left side of the pressure equation. In addition, the equations are discretized at the internal points, $i = 1, 3, \dots, n_x - 1$, $j = 1, 3, \dots, n_y - 1$ where, u_{ij}^{m+1} , v_{ij}^{m+1} and p_{ij}^{m+1} denotes the approximation of displacement u and v and pressure p in the spatial grid-point (x_i, y_j) at the temporal point t_{m+1} , where $m + 1$ indicate the current time step.

By using CDS to spatial approximations and reorganizing the terms, the Eq. (1) is written to $\mathbf{u} = (u, v)$ as follows

$$\begin{aligned} \frac{2(\lambda + 3\mu)}{h^2} u_{i,j}^{m+1} &= \frac{\lambda + 2\mu}{h^2} (u_{i-1,j}^{m+1} + u_{i+1,j}^{m+1}) + \frac{\mu}{h^2} (u_{i,j-1}^{m+1} + u_{i,j+1}^{m+1}) + \frac{\lambda + \mu}{4h^2} \\ &\quad (v_{i+1,j+1}^{m+1} - v_{i+1,j-1}^{m+1} - v_{i-1,j+1}^{m+1} - v_{i-1,j-1}^{m+1}) + \frac{1}{2h} (p_{i-1,j}^{m+1} - p_{i+1,j}^{m+1}) + f_{1,i,j}^{m+1} \end{aligned} \tag{5}$$

and

$$\begin{aligned} \frac{2(\lambda + 3\mu)}{h^2} v_{i,j}^{m+1} &= \frac{\lambda + \mu}{4h^2} \left(u_{i+1,j+1}^{m+1} - u_{i+1,j-1}^{m+1} - u_{i-1,j+1}^{m+1} + u_{i-1,j-1}^{m+1} \right) + \frac{\mu}{h^2} \\ &\left(v_{i-1,j}^{m+1} - v_{i+1,j}^{m+1} \right) + \frac{\lambda + 2\mu}{h^2} \left(v_{i,j-1}^{m+1} + v_{i,j+1}^{m+1} \right) + \frac{1}{2h} \left(p_{i,j-1}^{m+1} - p_{i,j+1}^{m+1} \right) + f_{2,i,j}^{m+1}. \end{aligned} \quad (6)$$

According to [32], to discretization of Eq. (2) we use

$$-\nabla \cdot (k(\mathbf{x}) \nabla p(\mathbf{x})) = c_{i,j}^h p_{i,j} + w_{i,j}^h p_{i-1,j} + e_{i,j}^h p_{i+1,j} + s_{i,j}^h p_{i,j-1} + n_{i,j}^h p_{i,j+1}, \quad (7)$$

where

$$w_{i,j}^h = -\frac{2}{h^2} \left(\frac{k_{i,j} k_{i-1,j}}{k_{i,j} + k_{i-1,j}} \right),$$

$$e_{i,j}^h = -\frac{2}{h^2} \left(\frac{k_{i,j} k_{i+1,j}}{k_{i,j} + k_{i+1,j}} \right),$$

$$s_{i,j}^h = -\frac{2}{h^2} \left(\frac{k_{i,j} k_{i,j-1}}{k_{i,j} + k_{i,j-1}} \right),$$

$$n_{i,j}^h = -\frac{2}{h^2} \left(\frac{k_{i,j} k_{i,j+1}}{k_{i,j} + k_{i,j+1}} \right),$$

$$c_{i,j}^h = -\left(w_{i,j}^h + e_{i,j}^h + n_{i,j}^h + s_{i,j}^h \right),$$

with $k_{i,j} = k(x_{i,j})$.

This way, using CDS and implicit Euler methods to, respectively, spatial and temporal approximations and assuming $\alpha = 1$ and $\beta \rightarrow \infty$ [30], the Eq. (2) is written as

$$\begin{aligned} \left(c_{i,j}^h + \frac{1}{(\lambda + 2\mu)\tau} \right) p_{i,j}^{m+1} + \left(w_{i,j}^h - \frac{1}{4(\lambda + 2\mu)\tau} \right) p_{i-1,j}^{m+1} + \left(e_{i,j}^h - \frac{1}{4(\lambda + 2\mu)\tau} \right) \\ p_{i+1,j}^{m+1} + \left(s_{i,j}^h - \frac{1}{4(\lambda + 2\mu)\tau} \right) p_{i,j-1}^{m+1} + \left(n_{i,j}^h - \frac{1}{4(\lambda + 2\mu)\tau} \right) p_{i,j+1}^{m+1} = \\ \frac{1}{2h\tau} \left(u_{i-1,j}^{m+1} - u_{i+1,j}^{m+1} + v_{i,j-1}^{m+1} - v_{i,j+1}^{m+1} + u_{i+1,j}^m - u_{i-1,j}^m + v_{i,j+1}^m - v_{i,j-1}^m \right) + \\ \frac{1}{4(\lambda + 2\mu)\tau} \left(4p_{i,j}^m - p_{i-1,j}^m - p_{i+1,j}^m - p_{i,j-1}^m - p_{i,j+1}^m \right) + g_{i,j}^{m+1}. \end{aligned} \quad (8)$$

The Equations (5), (6) and (8) corresponds to a large system of algebraic equations that needs to be solved efficiently.

3. Coarsening and smoothing strategy

The space-time multigrid method proposed here is an adaptation of that described in Franco et al. [1]. The space-time method with standard coarsening applied to the heat equation [1] does not converge if applied directly to the poroelasticity problem. Therefore, we describe here an adaptation to this method, where its components are based on an adaptive smoothing strategy that uses zebra-type relaxation on the planes xt , yt and standard coarsening using red-black fixed-stress smoother to multigrid method on the plane xy . That is, instead of using the red-black line-in-time relaxation, we should use space-time zebra on the planes xt and yt .

3.1. Coarsening strategy

The new space-time multigrid method (adapted from Franco et al. [1]) chooses a standard coarsening strategy to construct the grid-hierarchy, that is, the coarse-grid size doubles the fine-grid size in each direction (both temporal and spatial directions). Moreover, appropriate prolongation and restriction operators are chosen. In particular, the prolongation operator (I_{2h}^h) is chosen so that it does not transfer information backwards in time, whereas, the restriction operator (I_h^{2h}) is asymmetric and transferring no information forward in time. More concretely, these operators are given as follows

$$I_{2h}^h = \frac{1}{4} \begin{bmatrix} \left[\begin{array}{ccc} 0 & 0 & 0 \\ 0 & 0 & 0 \\ 0 & 0 & 0 \end{array} \right]_{2h}^h & \left[\begin{array}{ccc} 1 & 2 & 1 \\ 2 & 4 & 2 \\ 1 & 2 & 1 \end{array} \right]_{2h}^h & \left[\begin{array}{ccc} 1 & 2 & 1 \\ 2 & 4 & 2 \\ 1 & 2 & 1 \end{array} \right]_{2h}^h \end{bmatrix}, \tag{9}$$

$$I_h^{2h} = \frac{1}{32} \begin{bmatrix} \left[\begin{array}{ccc} 1 & 2 & 1 \\ 2 & 4 & 2 \\ 1 & 2 & 1 \end{array} \right]_{2h}^{2h} & \left[\begin{array}{ccc} 1 & 2 & 1 \\ 2 & 4 & 2 \\ 1 & 2 & 1 \end{array} \right]_{2h}^{2h} & \left[\begin{array}{ccc} 0 & 0 & 0 \\ 0 & 0 & 0 \\ 0 & 0 & 0 \end{array} \right]_{2h}^{2h} \\ \left[\begin{array}{ccc} 1 & 2 & 1 \\ 2 & 4 & 2 \\ 1 & 2 & 1 \end{array} \right]_h^{2h} & \left[\begin{array}{ccc} 1 & 2 & 1 \\ 2 & 4 & 2 \\ 1 & 2 & 1 \end{array} \right]_h^{2h} & \left[\begin{array}{ccc} 0 & 0 & 0 \\ 0 & 0 & 0 \\ 0 & 0 & 0 \end{array} \right]_h^{2h} \end{bmatrix}. \tag{10}$$

Notice that the previous stencil notation corresponds to a sequence of stencils applied to successive time-steps from the lowest (left stencil) to the highest (right stencil).

3.2. Smoothing strategy

An adaptive smoothing strategy is the key ingredient of the proposed space-time multigrid method with standard coarsening. Unlike Franco et al. [1] who combined different smoothers coupling with strong connections that depend on $\frac{\tau}{h^2}$ for choosing the smoother used in the multigrid method, in this work we use zebra smoothers in all directions, that is, xy , xt and yt . With that, regardless of the direction of the coupling, we guarantee that the multigrid method remains effective [33].

- *Scheme with zebra plane xt or zebra plane yt relaxation:* all variables of the xt or yt space-time planes are updated simultaneously using the block TDMA solver [34] and are visited by following a zebra-wise manner. In these updates, variables related to displacement and pressure in the x -lines and in each time step are exactly solved. The same process is done for the lines in the y -direction and at each time step. With that, we have the exact solutions of the planes xt or yt in each iterate.
- *Scheme with zebra plane-in-space relaxation:* all unknowns located at the same time-level are simultaneously updated, and the resulting planes are visited by following a zebra-wise manner. Theoretically, this smoother seems to be expensive due to the necessity of exactly solving the 2D problems arising from in plane relaxation. However, it is not necessary to solve them exactly, and it is sufficient to apply some multigrid cycles within each plane.

4. Results

In this section, we present some numerical experiments in order to demonstrate the robustness, efficiency and good performance of the space-time multigrid method proposed in previous section. We present some numerical experiments corresponding to two-dimensional poroelastic problems using $F(1, 1)$ -cycle. Rewriting Eqs. (5), (6) and (8) in the form $A\mathbf{w} = \mathbf{b}$, where A is the coefficient matrix, $\mathbf{w} = (u, v, p)$ and $\mathbf{b} = (f_1, f_2, g)$. This way, the residue is defined by $\mathbf{r} = \mathbf{b} - A\mathbf{w}$ [13]. The stopping criterion is given by $\frac{res^{mc}}{res^0} \leq 10^{-12}$, with

$$res^{mc} : = \|r_{u,h}^{mc}\|_{\infty} + \|r_{v,h}^{mc}\|_{\infty} + \|r_{p,h}^{mc}\|_{\infty}, \tag{11}$$

where $r_{u,h}^{mc}$, $r_{v,h}^{mc}$ and $r_{p,h}^{mc}$ indicate, respectively, the residues of u , v and p in h mesh after the mc -th multigrid cycle [35].

For scheme with zebra plane-in-space relaxation, we use $F(1, 1)$ -cycles for the plane relaxation until $\frac{res^{mc}}{res^0} \leq 10^{-2}$, since this multigrid cycle results in a very efficient space-time multigrid algorithm. In this $F(1,1)$ -cycle in spatial plane, the red-black fixed-stress split solver was used with red-black Gauss-Seidel [1]. In each iteration we smoothed 1 time the pressure p and 2 times the displacements u and v (see [19]).

The material properties of the porous medium are given by Young’s modulus and Poisson’s ratio, respectively, $E = 10^4$ and $\nu = 0.2$ [18, 19]. The final time $T = 1.0$ is considered in all simulations.

In order to illustrate a realistic $k(x, y)$ for real world problems on a calculation domain composed of materials that have random hydraulic conductivity, according to [32], we consider a reference parameters set, here called Matérn, $\Phi = (\nu_c, \lambda_c, \sigma_c^2)$ that are related to Gaussian random fields. Where the parameter ν_c defines the field smoothness, σ_c^2 represents its variance and λ_c is the correlation length of the covariance function. Moreover, parameters λ_c and σ_c^2 prescribe the number of peaks and the amplitude of the random field, respectively.

Considering the spatial square domain $\Omega = (0, 1) \times (0, 1)$ and the highest order of complexity [33], $\nu_c = 0.5$, $\lambda_c = 0.1$ and $\sigma_c^2 = 3$, i.e. $\Phi = (0.5, 0.1, 3)$, here called $\Phi_4 = (0.5, 0.1, 3)$, the random hydraulic conductivity field generated with these Matérn parameters set, sampled on a uniform mesh, are presented in Figure 1. The respective minimum and maximum values of $k(x, y)$, k_1 and k_2 , described in Figure 1, considering $n_x = n_y$, are presented in Table 1, where they have already been multiplied, respectively by 10^{-8} and 10^{-4} , to obtain realistic values. In order to obtain the value of $k(x, y)$ on the coarse grids in the multigrid method, we use the full-weighting restriction process (see [13]).

In order to show the robustness of the method with respect to the physical and discretization parameters, we show in the Figure 2 the average convergence factor (ρ_m) obtained after using $F(1, 1)$ -cycle until reaching the stop criterion. Note that, regardless of the mesh refinement, ρ_m is roughly constant, thus indicating the robustness of the method. Furthermore, we obtain good ρ_m for every cases, i.e. the ρ_m are small.

Note in Figure 3 an excellent error decay in each $F(1, 1)$ multigrid cycle performed, considering $n_x = n_y = n_t = 2^9$.

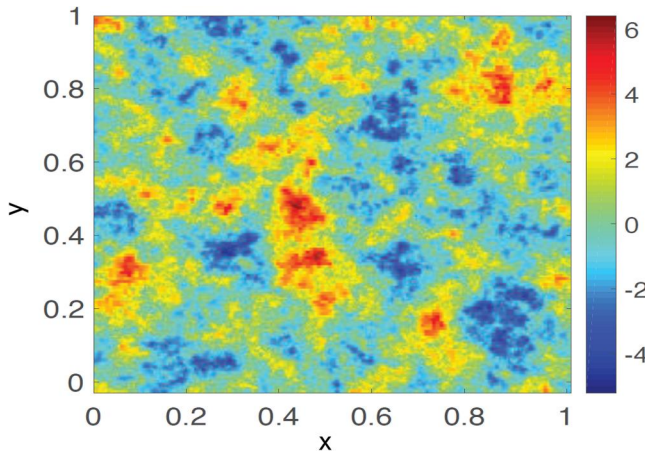


Figure 1. Logarithm of the conductivity field, $\log k$, generated using $\Phi_4 = (0.5, 0.1, 3)$ [32, p. A1400].

Table 1. Minimum (k_1) and maximum (k_2) of $k(x, y)$ multiplied by 10^{-8} and 10^{-4} and using $\Phi_4 = (0.5, 0.1, 3)$.

$n_x = n_y$	$k(x, y) \cdot 10^{-8}$		$k(x, y) \cdot 10^{-4}$	
	k_1	k_2	k_1	k_2
2^3	1.92E-10	1.20E-07	1.92E-06	1.20E-03
2^4	9.59E-11	5.13E-07	9.59E-07	5.13E-03
2^5	1.02E-10	6.58E-07	1.02E-06	6.58E-03
2^6	1.94E-11	1.58E-06	1.94E-07	1.58E-02
2^7	7.85E-12	6.92E-06	7.85E-08	6.92E-02
2^8	2.37E-11	1.08E-05	2.37E-07	1.08E-01
2^9	4.55E-11	1.11E-05	4.55E-07	1.11E-01

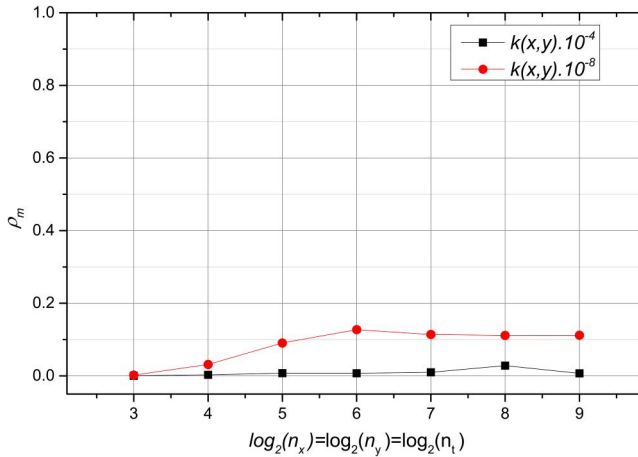


Figure 2. Average convergence factors (ρ_m) in different grid-sizes to $k(x, y) \cdot 10^{-8}$ and $k(x, y) \cdot 10^{-4}$ using $F(1, 1)$ multigrid cycles and $\frac{res^{mc}}{res^0} \leq 10^{-12}$ as stopping criterion.

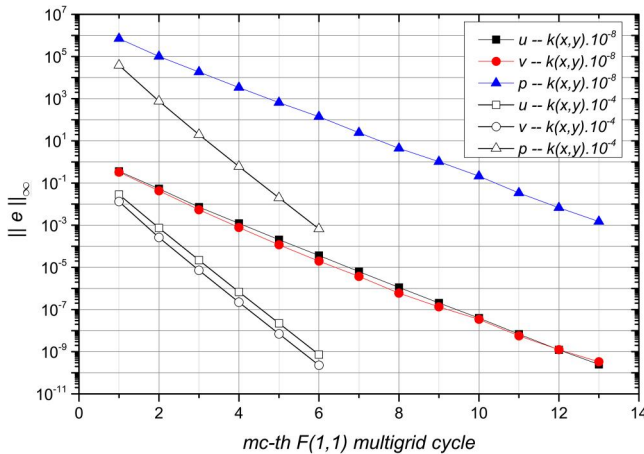


Figure 3. Numerical error to u, v and p in different $F(1, 1)$ multigrid cycles (mc) to $k(x, y) \cdot 10^{-8}$ and $k(x, y) \cdot 10^{-4}$ and $\frac{res^{mc}}{res^0} \leq 10^{-12}$ as stopping criterion.

Corroborating with the results described in the [Figure 2](#) and [Figure 3](#), the [Table 2](#) shows the number of $F(1, 1)$ multigrid cycles (nmc) necessary to reduce the maximum norm of the initial residual until the required tolerance (by a factor of 10^{-12}) and the respective average convergence factor. The results are shown for values of random hydraulic conductivity $k(x, y)$ multiplied by

Table 2. Number of $F(1, 1)$ multigrid cycles required to reduce the maximum norm of the initial residual by a factor of 10^{-9} for different grid-sizes with $n_x = n_y = 2^7$ points.

$n_x = n_y$	$k(x, y) \cdot 10^{-8}$		$k(x, y) \cdot 10^{-4}$	
	nmc	ρ_m	nmc	ρ_m
2^7	13	1.14E-01	6	9.97E-03
2^8	14	1.25E-01	7	1.91 E-02
2^9	14	1.37E-01	9	3.92 E-02
2^{10}	15	1.56E-01	10	5.39 E-02
2^{11}	16	1.70E-01	11	8.03 E-02
2^{12}	16	1.73E-01	13	1.09 E-01
2^{13}	16	1.74E-01	14	1.32E-01

10^{-8} and 10^{-4} , and for different grid-sizes. The number of spatial steps are fixed as $n_x = n_y = 2^7$, whereas different numbers of time-steps are considered $2^7 \leq n_t \leq 2^{13}$. Even assuming random $k(x, y)$, we can observe the robustness of the proposed method, which provides very satisfactory values.

5. Conclusions

In this work, we proposed a robust space-time multigrid method combining standard coarsening with the selection of suitable solvers/smoother for solving the poroelasticity equations with random hydraulic conductivity. To achieve convergence, it was necessary to use zebra-type solvers, where for the temporal planes the TDMA block method was used, while in the spatial plane some F -cycles of the multigrid were used. Two-dimensional space for the spatial and temporal approximations of the problems was considered, using, respectively, central differences and implicit Euler methods. The method demonstrated excellent convergence rates across a wide range of random hydraulic conductivity values, showcasing its robustness and efficiency. This shows that the space-time multigrid method proposed, besides being highly parallelizable, makes it a powerful tool for efficiently solving poroelasticity problems, including those with random hydraulic conductivity. Furthermore, this approach can be extended to semi-structured meshes, that is, globally unstructured, but locally structured meshes.

Disclosure statement

No potential conflict of interest was reported by the author(s).

ORCID

Sebastião Romero Franco  <http://orcid.org/0000-0002-4580-5924>

Marcio Augusto Villela Pinto  <http://orcid.org/0000-0003-4166-4674>

References

- [1] S. R. Franco, F. J. Gaspar, M. A. V. Pinto and C. Rodrigo, "Multigrid method based on a space-time approach with standard coarsening for parabolic problems," *Appl. Math. Comput.*, vol. 317, pp. 25–34, 2018. DOI: [10.1016/j.amc.2017.08.043](https://doi.org/10.1016/j.amc.2017.08.043).
- [2] F. J. Gaspar, F. J. Lisbona, C. W. Oosterlee and R. Wienands, "A systematic comparison of coupled and distributive smoothing in multigrid for the poroelasticity system," *Numerical Linear Algebra App.*, vol. 11, no. 2–3, pp. 93–113, 2004. DOI: [10.1002/nla.372](https://doi.org/10.1002/nla.372).
- [3] M. A. Biot, "Theory of elasticity and consolidation for a porous anisotropic solid," *J. Appl. Phys.*, vol. 26, no. 2, pp. 182–185, 1955. DOI: [10.1063/1.1721956](https://doi.org/10.1063/1.1721956).
- [4] F. Vermolen, C. Rodrigo, F. Gaspar and K. Kumar, "Guest editorial to the special issue: computational mathematics aspects of flow and mechanics of porous media: state-of-the-art computational methods in the

- mechanics and flow in porous media,” *Comput Geosci*, vol. 25, no. 2, pp. 601–602, 2021. DOI: [10.1007/s10596-021-10047-0](https://doi.org/10.1007/s10596-021-10047-0).
- [5] R. L. Burden and J. D. Faires, *Numerical Analysis*, 10th ed. Boston: Cengage Learning, 2016.
- [6] L. Zhang, J. Ba and J. Carcione, “Wave propagation in infinituple-porosity media,” *J. Geophys. Research: Solid Earth*, vol. 126, no. 4, pp. 1–19, 2021. DOI: [10.1029/2020JB021266](https://doi.org/10.1029/2020JB021266).
- [7] J. Santos, P. Gauzellino, J. Carcione and J. Ba, “Effective viscoelastic representation of gas-hydrate bearing sediments from finite-element harmonic experiments,” *Comput Geosci*, vol. 25, no. 6, pp. 2005–2017, 2021. DOI: [10.1007/s10596-021-10077-8](https://doi.org/10.1007/s10596-021-10077-8).
- [8] J. Santos, J. Carcione, G. Savioli and J. Ba, “Wave propagation in thermo-poroelasticity: a finite-element approach,” *Geophys*, vol. 88, no. 1, pp. WA161–WA175, 2023. DOI: [10.1190/geo2022-0271.1](https://doi.org/10.1190/geo2022-0271.1).
- [9] C. D. Santiago, G. R. Ströher, M. A. V. Pinto and S. R. Franco, “A multigrid waveform relaxation method for solving the Pennes bioheat equation,” *Numer. Heat Transf. A: Appl*, vol. 83, no. 9, pp. 976–990, 2023. DOI: [10.1080/10407782.2022.2156411](https://doi.org/10.1080/10407782.2022.2156411).
- [10] M. F. Malacarne, M. A. V. Pinto and S. R. Franco, “Performance of the multigrid method with time-stepping to solve 1D and 2D wave equations,” *Int. J. Comput. Meth. Eng. Sci. Mech*, vol. 23, no. 1, pp. 45–56, 2022. DOI: [10.1080/15502287.2021.1910750](https://doi.org/10.1080/15502287.2021.1910750).
- [11] J. M. B. Oliveira, L. K. Araki, M. A. V. Pinto and S. F. T. Gonçalves, “An alternative full multigrid simplec approach for the incompressible Navier-Stokes equations,” *Numer. Heat Transf. B: Fundam*, vol. 83, no. 6, pp. 410–432, 2023. DOI: [10.1080/10407790.2023.2167752](https://doi.org/10.1080/10407790.2023.2167752).
- [12] F. J. Gaspar, F. J. Lisbona and P. N. Vabishchevich, “Staggered grid discretizations for the quasi-static Biot’s consolidation problem,” *Appl. Numer. Math*, vol. 56, no. 6, pp. 888–898, 2006. DOI: [10.1016/j.apnum.2005.07.002](https://doi.org/10.1016/j.apnum.2005.07.002).
- [13] U. Trottenberg, C. Oosterlee and A. Schüller, *Multigrid*. San Diego: Academic Press, 2001,
- [14] P. Wesseling, *An Introduction to Multigrid Methods*. Chichester: John Wiley & Sons, 1992,
- [15] F. Oliveira, S. R. Franco and M. A. V. Pinto, “The effect of multigrid parameters in a 3D heat diffusion equation,” *Int. J. Appl. Mech. Eng*, vol. 23, no. 1, pp. 213–221, 2018. DOI: [10.1515/ijame-2018-0012](https://doi.org/10.1515/ijame-2018-0012).
- [16] C. W. Oosterlee and P. Wesseling, “A multigrid method for an invariant formulation of the incompressible Navier-Stokes equations in general coordinates,” *Commun. appl. numer. methods*, vol. 8, no. 10, pp. 721–734, 1992. DOI: [10.1002/cnm.1630081003](https://doi.org/10.1002/cnm.1630081003).
- [17] C. Oosterlee and P. Wesseling, “A robust multigrid method for a discretization of the incompressible Navier-Stokes equations in general coordinates,” *IMPACT Comput. Sci. Eng*, vol. 5, no. 2, pp. 128–151, 1993. DOI: [10.1006/icse.1993.1006](https://doi.org/10.1006/icse.1993.1006).
- [18] F. J. Gaspar, F. J. Lisbona, C. W. Oosterlee and P. N. Vabishchevich, “An efficient multigrid solver for a reformulated version of the poroelasticity system,” *Comput. Meth. Appl. Mech. Eng*, vol. 196, no. 8, pp. 1447–1457, 2007. DOI: [10.1016/j.cma.2006.03.020](https://doi.org/10.1016/j.cma.2006.03.020).
- [19] F. J. Gaspar and C. Rodrigo, “On the fixed-stress split scheme as smoother in multigrid methods for coupling flow and geomechanics,” *Comp. Meth. Appl. Mech. Eng*, vol. 326, pp. 526–540, 2017. DOI: [10.1016/j.cma.2017.08.025](https://doi.org/10.1016/j.cma.2017.08.025).
- [20] P. Luo, C. Rodrigo, F. Gaspar and C. Oosterlee, “Monolithic multigrid method for the coupled Stokes flow and deformable porous medium system,” *J. Comput. Phys*, vol. 353, pp. 148–168, 2018. DOI: [10.1016/j.jcp.2017.09.062](https://doi.org/10.1016/j.jcp.2017.09.062).
- [21] S. Saberi, G. Meschke and A. Vogel, “A restricted additive Vanka smoother for geometric multigrid,” *J. Comput. Phys*, vol. 459, pp. 111123, 2022. DOI: [10.1016/j.jcp.2022.111123](https://doi.org/10.1016/j.jcp.2022.111123).
- [22] P. Luo, C. Rodrigo, F. J. Gaspar and C. W. Oosterlee, “Uzawa smoother in multigrid for the coupled porous medium and Stokes flow system,” *SIAM J. Sci. Comput*, vol. 39, no. 5, pp. S633–S661, 2017. DOI: [10.1137/16M1076514](https://doi.org/10.1137/16M1076514).
- [23] M. J. Gander and M. Neumüller, “Analysis of a new space-time parallel multigrid algorithm for parabolic problems,” *SIAM J. Sci. Comput*, vol. 38, no. 4, pp. A2173–A2208, 2016. DOI: [10.1137/15M1046605](https://doi.org/10.1137/15M1046605).
- [24] R. Falgout, *et al.*, “Multigrid methods with space-time concurrency,” *Comput. Visual Sci*, vol. 18, no. 4–5, pp. 123–143, 2017. DOI: [10.1007/s00791-017-0283-9](https://doi.org/10.1007/s00791-017-0283-9).
- [25] G. Horton and S. Vandewalle, “A space-time multigrid method for parabolic partial differential equations,” *SIAM J. Sci. Comput*, vol. 16, no. 4, pp. 848–864, 1995. DOI: [10.1137/0916050](https://doi.org/10.1137/0916050).
- [26] R. D. Falgout, S. Friedhoff, T. V. Kolev, S. P. MacLachlan and J. B. Schroder, “Parallel time integration with multigrid,” *SIAM J. Sci. Comput*, vol. 36, no. 6, pp. C635–C661, 2014. DOI: [10.1137/130944230](https://doi.org/10.1137/130944230).
- [27] M. Emmett and M. L. Minion, “Toward an efficient parallel in time method for partial differential equations,” *CAMCoS*, vol. 7, no. 1, pp. 105–132, 2012. DOI: [10.2140/camcos.2012.7.105](https://doi.org/10.2140/camcos.2012.7.105).
- [28] J.-L. Lions, Y. Maday and G. Turinici, “A ‘parareal’ in time discretization of PDE’s,” *Comptes Rendus de l’Académie des Sciences, Série I. Mathématique*, vol. 332, pp. 661–668, 2001. DOI: [10.1016/S0764-4442\(00\)01793-6](https://doi.org/10.1016/S0764-4442(00)01793-6).

- [29] M. J. Gander and S. Vandewalle, “Analysis of the parareal time parallel time-integration method,” *SIAM J. Sci. Comput.*, vol. 29, no. 2, pp. 556–578, 2007. DOI: [10.1137/05064607X](https://doi.org/10.1137/05064607X).
- [30] S. R. Franco, C. Rodrigo, F. J. Gaspar and M. A. V. Pinto, “A multigrid waveform relaxation method for solving the poroelasticity equations,” *Comp. Appl. Math.*, vol. 37, no. 4, pp. 4805–4820, 2018. DOI: [10.1007/s40314-018-0603-9](https://doi.org/10.1007/s40314-018-0603-9).
- [31] C. W. Oosterlee and F. J. Gaspar, “Multigrid relaxation methods for systems of saddle point type,” *Appl. Numer. Math.*, vol. 58, no. 12, pp. 1933–1950, 2008. DOI: [10.1016/j.apnum.2007.11.014](https://doi.org/10.1016/j.apnum.2007.11.014).
- [32] P. Kumar, C. Rodrigo, F. Gaspar and C. Oosterlee, “On local Fourier analysis of multigrid methods for PDEs with jumping and random coefficients,” *SIAM J. Sci. Comput.*, vol. 41, no. 3, pp. A1385–A1413, 2019. DOI: [10.1137/18M1173769](https://doi.org/10.1137/18M1173769).
- [33] C.-A. Thole and U. Trottenberg, “Basic smoothing procedures for the multigrid treatment of elliptic 3D operators,” *Appl. Math. Comput.*, vol. 19, no. 1–4, pp. 333–345, 1986. DOI: [10.1016/0096-3003\(86\)90112-8](https://doi.org/10.1016/0096-3003(86)90112-8).
- [34] N. J. Scenna, “Sistemas de ecuaciones de gran dimensión y poco densos,” in *Modelado, simulación y optimización de procesos químicos*. Buenos Aires, Argentina: Universidad Tecnológica Nacional, 1999, pp. 117–189.
- [35] R. Wienands, F. J. Gaspar, F. J. Lisbona and C. W. Oosterlee, “An efficient multigrid solver based on distributive smoothing for poroelasticity equations,” *Comput.*, vol. 73, no. 2, pp. 99–119, 2004. DOI: [10.1007/s00607-004-0078-y](https://doi.org/10.1007/s00607-004-0078-y).